Modeling Earth Systems and Environment (2022) 8:309–322
https://doi.org/10.1007/s40808-020-01079-z

ORIGINAL ARTICLE

Assessing impact of urbanisation on surface runoff using vegetation-impervious surface-soil (V-I-S) fraction and NRCS curve number (CN) model

Debarati Bera[1] · Pramod Kumar[1] · Asfa Siddiqui[1] · Anwesha Majumdar[1]

Received: 30 May 2020 / Accepted: 30 December 2020 / Published online: 19 January 2021

Abstract
The progressive decrease in natural surfaces to create space for urban dwellers with the consequential changes caused to hydrological regime of an area is taking a toll on environmental resources. The Natural Resources Conservation Service (NRCS) Curve Number (CN) model (earlier known as Soil Conservation Service Curve Number, SCS-CN) is used in the present study for assessing temporal variations in surface runoff in upper catchment of Rispana River, Dehradun city, India. Also, the composite CN is calculated using vegetation-impervious surface-soil (V-I-S) fraction derived from spectral normalisation and linear spectral mixture analysis method while assigning initial CN for hydrologic soil-cover complex for five years during 1991 to 2018. The results indicated a steady rise in impervious surface fraction and consequent surface runoff (8.25%) from 1991 to 2018, while urban green space fraction has shown depleting trends in north and central part of the city. The level of imperviousness highlighted an over 60% of central part of the city as impervious, which gradually decreases outwards from the city. A positive correlation is observed between surface runoff and ISA (R^2 varies between 0.62 and 0.89, $p < 0.05$), whereas inverse relationship is observed with vegetative cover in all sub-basins (R^2 varies between 0.61 and 0.91, $p < 0.05$). The study demonstrates the potential of NRCS-CN model with inputs drawn from V-I-S fraction for simulating surface runoff and understanding the urban flood risk. The work would be useful for the urban dwellers, administrators and planners for better planning and sustainable development of urban areas.

Keywords NRCS-CN · V-I-S · LSMA · Surface runoff · Urbanisation

Introduction

In the existing global scenario of depleting water resources due to deforestation and other anthropogenic activities, the importance of understanding the relationship between rainfall and surface runoff and its trend holds vital significance in a monsoon dominated landmass of India and other parts of the world. With 31.8% urbanisation, India is progressively showing symptoms of modified landscapes, primarily in the urban sector, in both core and fringe areas (Census of India 2011). The dramatic reduction in pervious surfaces (urban green and open spaces, water bodies, etc.) in urban areas is posing a risk of increased surface runoff aggravated through poor storm-water management, especially during peak rainfall event (Weng 2012; Gnecco et al. 2018). This ultimately leads to water logging and several other consequent effects to the inhabitants living in the vicinity. It is imperative to estimate the direct surface runoff which is subject to changes in land cover, socio-economic drivers and other hydrological processes for environmental impact analysis (Dutta et al. 2006; Gupta et al. 2019).

The use of geospatial data and related techniques provides a gambit of temporal, spectral and spatial information and has reduced the time and efforts put into the manual methods of runoff estimation and flood modelling (Lu and Weng 2009; Samah et al. 2009; Fan et al. 2013; Phetprayoon 2015). Remote sensing data-based hydrological modelling techniques (Abdulkareem et al. 2018) embedded in Hydrologiska Byråns Vattenbalansavdelning (HBV) model (Bergstrom 1995), Sacramento model (Burnash 1995), Tank model (Sugawara 1995), Soil and Water Assessment Tool

✉ Asfa Siddiqui
asfa.aas@gmail.com; asfa@iirs.gov.in

[1] Urban and Regional Studies Department, Indian Institute of Remote Sensing, Indian Space Research Organisation, 4-Kalidas Road, Dehradun, Uttarakhand 248001, India

(SWAT) model (Arnold et al. 1998; Hörmann et al. 2009; Neitsch et al. 2011; Kumar et al. 2016), CASC2D (Downer et al. 2002), HEC-HMS model (Kousari et al. 2010; US Army Corps of Engineers 2018; Cahyono and Adidarma 2019; Meresa 2019), etc. have been used in various studies with varied datasets for urban surface runoff estimation and flood risk modelling. The characteristic spatio-temporal availability of medium resolution imagery giving pixel-level information facilitates the precise feature identification and mapping (Fortin et al. 2001; Blaschke et al. 2011). Among the widely used methods, the Natural Resources Conservation Service (NRCS) earlier known as Soil Conservation Service (SCS) curve number (CN) model developed by the United States Department of Agriculture (USDA) is a widely accepted and used method for estimating the direct surface runoff against a specific rainfall event (Velásquez-Valle et al. 2017). The NRCS model's parameter, i.e. curve number (CN), details out the surface runoff depth and is greatly influenced by land use, soil and moisture conditions of soil (Fan et al. 2013; Al-Ghobari et al. 2020; Caletka et al. 2020; Karunanidhi et al. 2020; Nageswara Rao 2020; Psomiadis et al. 2020; Shi and Wang 2020; Verma et al. 2020; Walega et al. 2020) indicating the surface runoff. The CN values for various hydrological soil groups (HSGs) are given in standardised format in USDA Technical Release 55 (TR-55) lookup table (USDA Natural Resources Conservative Centre 1986). Studies have indicated that the classes mentioned in TR-55 do not hold well when working on medium-resolution imageries, and hence, infiltration parameters like impervious surface area (ISA) can be readily used as a proxy to estimate the CN. The SCS-CN model has been modified based on regional- and local-level variations to improve the surface runoff simulations specifically for urban areas (Gao et al. 2012; Ajmal et al. 2015, 2016; Rajbanshi 2016). After the antecedent moisture conditions (AMC) is adjusted in the SCS-CN model, it is a model preferred for surface runoff simulation. Ludlow (2009) and Fan et al. (2013) developed a technique to calculate the composite CN by integrating the vegetation-impervious surface-soil (V-I-S) fraction (Ridd 1995; Fan et al. 2013) based on normalised spectral mixture analysis (NSMA) and linear spectral mixture analysis (LSMA) methods (Lu and Weng 2006; Weng and Hu 2008; Fan et al. 2015; Yang and He 2017). Zhang et al. (2015) and Fan et al. (2013) applied the composite CN method to estimate urban surface runoff in different cities using remote sensing datasets and have concluded its effectiveness over conventional methods (Reistetter and Russell 2011; Fan et al. 2013; Kowalik and Walega 2015; Wałęga and Rutkowska 2015; Zhang et al. 2015; Ajmal et al. 2016).

This study focuses on estimating the composite CN using V-I-S fraction (Ridd 1995) while dividing the study area into impervious surface, soil and vegetation classes. The abundance image obtained through the unmixing technique is calculated using Landsat TM, ETM + and OLI datasets of 5 years (1991, 1998, 2003, 2011 and 2018) to explain the temporal effects of urbanisation and its impact on surface runoff (Wu and Murray 2003; Lu and Weng 2013). The initial CN values derived through the TR-55 lookup table and keeping in mind the soil and vegetation dynamics within study area have helped in estimating the composite CN. Sub-watershed-wise surface runoff was computed in Hydrologic Engineering Center–Hydrologic Modeling System (HEC-HMS) using the extreme event (Natarajan and Radhakrishnan 2019) of last 30 years based on monthly Standardized Precipitation Index (SPI-1). According to SPI-1, September 2010 was identified as an extreme wet month (SPI > 2.5) and one of the extreme events occurred on 20 September 2010 with 149.3 mm rainfall was used in the present study. Thus, the impact of urban growth on direct surface runoff using the composite CN method embedded in SCS-CN model was analysed for different sub-watersheds within the upper catchment of Rispana River in Dehradun city, India.

Material and methods

Study area

The present study is carried out for the upstream catchment of Rispana River in Dehradun city, Uttarakhand State, India. The geographical extent of study area lies between 30° 13′ N to 30° 27′ N latitude and 77° 58′ E to 78° 06′ E longitude (Fig. 1) with an area of about 120 km^2. It has an undulating terrain with the altitudinal variation ranging from 600 m (in the southern part) to 2235 m (in the northern side) above mean sea level. The study area is dominated by the humid subtropical climate and the majority of rainfall is received during June–September months due to southwest monsoon. The annual average rainfall is about 2183.5 mm. During the winter months, the minimum temperature varies between 2 and 5 °C whereas the maximum temperature in summer months ranges from 40 to 43 °C. Within such kind of vulnerable landscape and socio-economic conditions, a large population reside within the Dehradun city (5.78 lakh inhabitants as per Census of India 2011) supported with social and physical infrastructure (Census of India 2011). The study area has varying landscapes and consists mainly of urban and peri-urban built-up areas, natural and artificial vegetation cover and different soil types.

Data used

Landsat-5 TM ETM + and OLI images (Path 146/Row 39) of five time periods, viz. 1991, 1998, 2003, 2011 and 2018, procured from United States Geological Survey (USGS) website were used for performing the NSMA and retrieving the

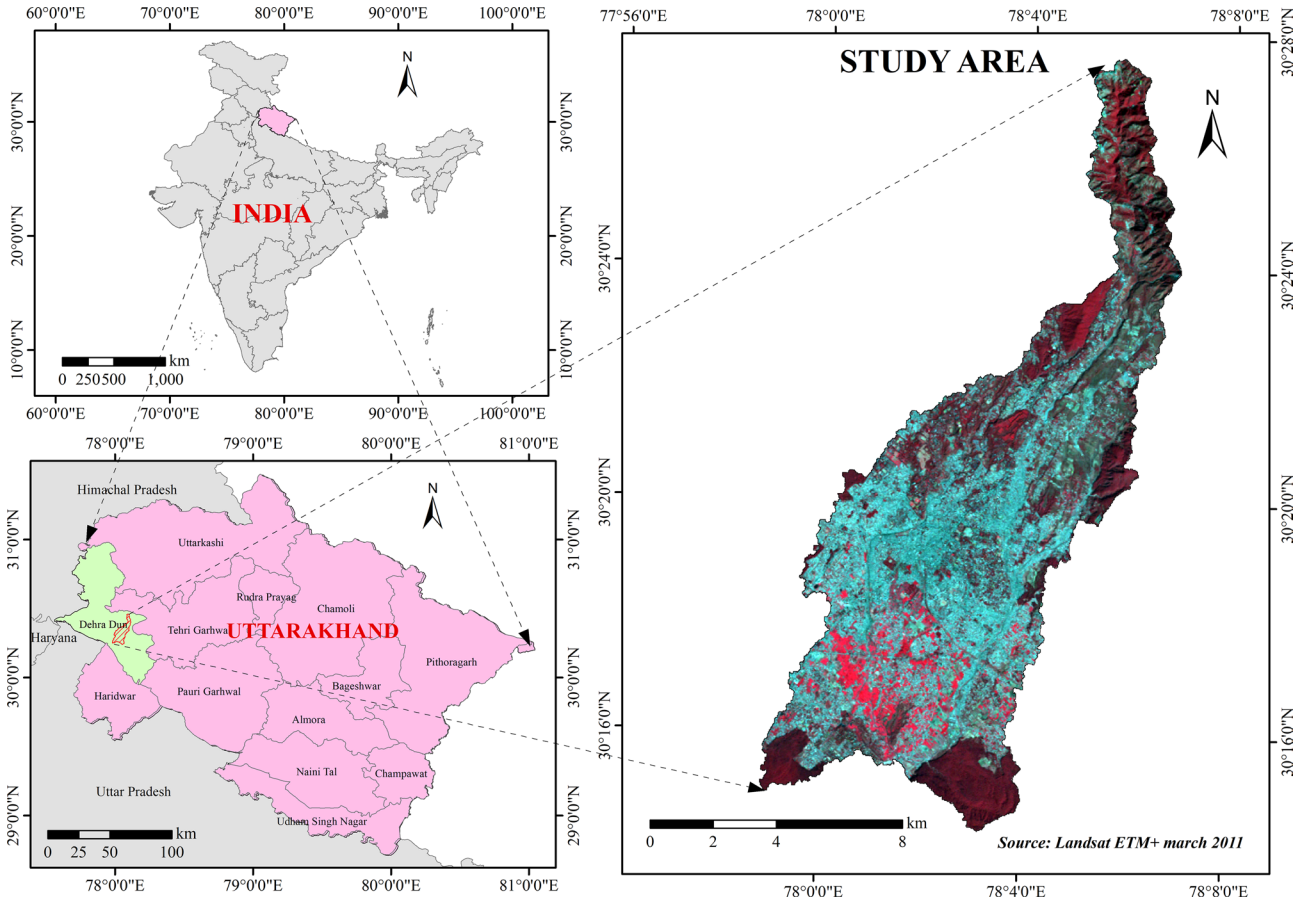

Fig. 1 Study Area

V-I-S fraction maps. Landsat datasets were atmospherically corrected using Fast Line-of-sight Atmospheric Analysis of Spectral Hypercubes (FLAASH) which is a MODerate-resolution atmospheric TRANsmission (MODTRAN)-based atmospheric correction model and reflectance values were obtained for all the bands. In addition to this, the Shuttle Radar Topography Mission (SRTM) Digital Elevation Model (DEM) was used for preparing the slope map of the area. The soil map of the study area prepared by National Bureau of Soil Survey and Land Use Planning (NBSS and LUP) at 1:5,00,000 scale has been used to understand the soil types. The rainfall data of 30 years (1982–2012) have been used for the computation of surface runoff collected from Indian Meteorological Department (IMD).

General methodology

An overall methodology adopted in the study is presented in Fig. 2. The satellite data from Landsat TM, ETM + and OLI for years 1991, 1998, 2003, 2011 and 2018 were atmospherically corrected using FLAASH correction model. Thus, the noises in the form of atmospheric components like water vapour, aerosols and other gaseous particles were removed. The catchment area was delineated as study area using SRTM DEM and the fill sinks, flow direction, flow accumulation, stream definition and segmentation analyses were performed. The catchment grids were delineated and with vectorised feature classes, the watershed and sub-watersheds were delineated. Subsequently, Normalised Difference Vegetation Index (NDVI) was calculated for the temporal datasets. The impervious surface area was calculated using the LSMA and the soil map of the study area was regrouped to produce the HSG map. Later, the composite CN was estimated using percentage of ISA, HSG and vegetation class as discussed in the following sections (Figs. 3, 4, 5, 6 and 7).

Extracting the V-I-S components using LSMA technique

The CN is calculated after obtaining the fractional map of impervious surface area and derived using a linear unmixing approach normalised for the extraction of features. Procedurally, the reflectance values of all bands are normalised first for minimising the difference between high,

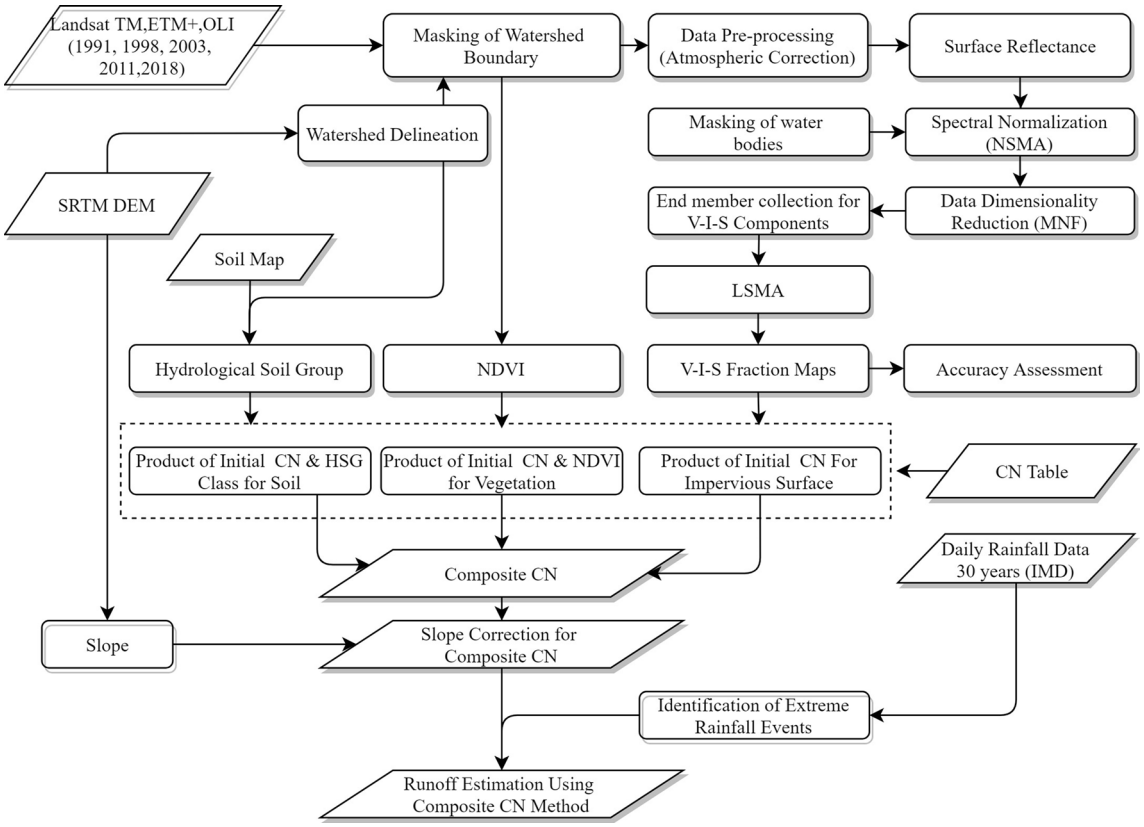

Fig. 2 Flowchart of adopted methodology

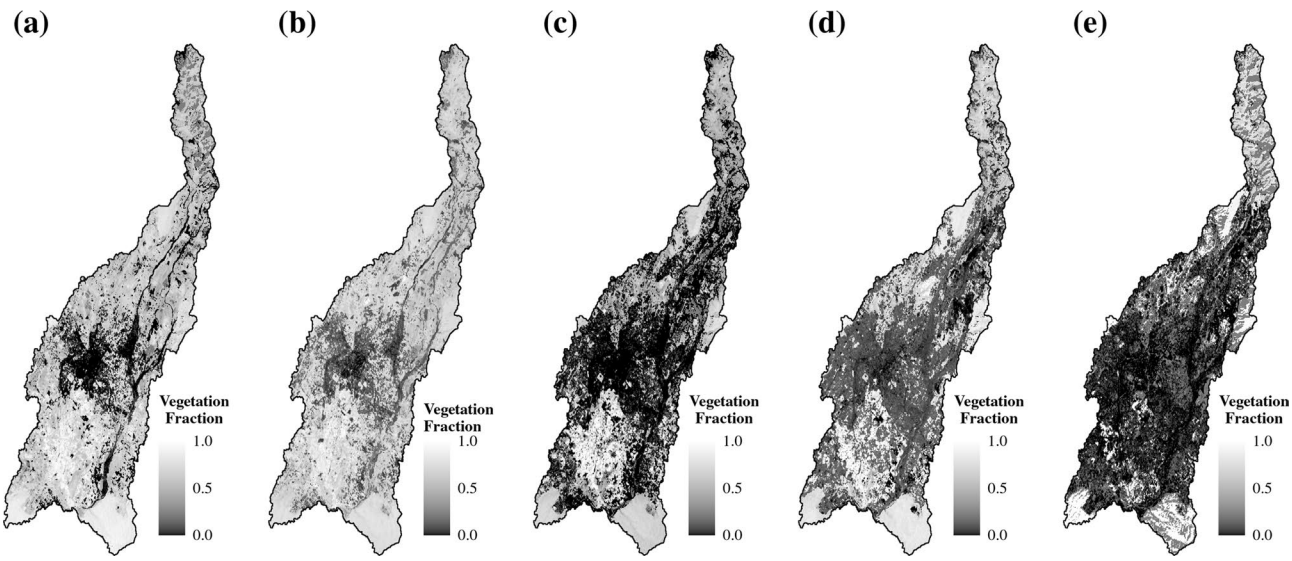

Fig. 3 Vegetation fraction map **a** 1991 **b** 1998 **c** 2003 **d** 2011 and **e** 2018

medium and low albedo pixels belonging to three classes, viz. vegetation, impervious surface and soil. This procedure is followed by masking out the water pixels for better results. Hence, shape information can be highlighted using the normalisation technique that minimises the absolute reflectance values using a normalisation method (Eq. 1) given as follows:

$$\hat{R}_b = \frac{R_b}{\mu} \times 100, \tag{1}$$

and

$$\mu = \frac{1}{N} \sum_{b=1}^{N} R_b, \tag{2}$$

where $\hat{R}_b$ is the normalised reflectance for band 'b' in a pixel, R_b is the original reflectance for band 'b', μ is the average reflectance for that pixel and N is the total number of bands (6 for TM image). The internal variation observed within different land cover types is now minimised when compared to the original image bearing the enhanced reflectance values. The minimum noise fraction (MNF) transformation is carried out to select the required endmembers after applying the linear unmixing on the normalised bands (Pal et al. 2011; Kumar et al. 2019). Through the normalised inverse MNF image, the LSMA was performed. The accurate quantitative information is extracted as sub-pixel level through the LSMA technique (Roberts et al. 1998). LSMA is based on an assumption that the spectrum value is a linear combination of the sum of all values pertaining to all land cover types (or endmembers) associated with the pixel. The mathematical model (Eq. 3) of LSMA can be expressed as:

$$R_i = \sum\nolimits_{k=1}^{n} {}_k R_{ik} + \mathrm{ER}_i, \tag{3}$$

where, $i = 1, \ldots, m$ (number of spectral bands), $k = 1, \ldots, n$ (number of endmembers), R_i is the spectral reflectance of band i which contains endmembers, $\int(k)$ is the proportion of endmember k within the pixel, R_{ik} is the known spectral reflectance of endmember k within the pixel on band i and ER_i is the error for band i (Ridd 1995; Wu 2004). The hydrologic soil-cover complex represented by major classes in an urban area, viz. vegetation, impervious surface and soil, can be used in V-I-S model. The first three MNF components containing 90% of the original information were used for extracting endmembers through the image-based endmember extraction method. The three (V-I-S) fraction maps for five different years were extracted from the normalised values. The accuracy of results was assessed using high-resolution Google Earth imagery. A total of 101 polygons (100 m × 100 m) within uniformly distributed locations in the study area were randomly selected representing the three major V-I-S components (Figs. 3, 4 and 5). These components were separately digitised in Google Earth imagery and proportions were identified from LSMA-derived components for comparison. The root mean square error (RMSE) and bias was calculated subsequently.

Estimating the composite curve number (CN)

The V-I-S fraction maps have been prepared using the LSMA model and later combined with the NDVI and soil types of the study area for the estimation of composite curve number of the urban and peri-urban areas. Initially, the soil type and NDVI images were reclassified into the desired classes. Subsequently, the percentage of ISA (Fig. 4), NDVI(Fig. 6) and soil class (Fig. 5) were assessed which helped in calculating the CN (Fig. 7). Each of the soil classes was allocated an initial $\mathrm{CN_S}$ value in reference to the TR-55 (Table 1) based on HSG class. The study area is governed by two major HSGs, namely B and C. The initial $\mathrm{CN_V}$ threshold for vegetation class was estimated based on the classification of NDVI image (Fig. 6). The NDVI value was broadly divided into four categories as follows: (a) NDVI > 0.62 representing forest land, (b) NDVI ranging from 0.55 to 0.62 representing orchards, (c) NDVI ranging from 0.31 to 0.55 as grass and farmland and (d) NDVI < 0.31 representing non-vegetated areas. Each range is further subdivided into classes indicating the poor, fair and good condition of vegetation depending on the abundance values in each pixel assessed through vegetation component in V-I-S fraction map as indicated in Table 2. The impervious surfaces are the areas where

Table 1 Value of initial $\mathrm{CN_S}$ and corresponding HSG

Vegetation	NDVI	Vegetation Health	CN			
			A	B	C	D
Forest	NDVI > 0.62	Poor (V < 50%)	45	66	77	83
		Fair (50% < V < 75%)	36	60	73	79
		Good (> 75%)	25	55	70	77
Orchards	0.55 < NDVI < 0.62	Poor (V < 50%)	57	73	82	86
		Fair (50% < V < 75%)	43	65	76	82
		Good (> 75%)	32	58	72	79
Grass and Farmland	0.31 < NDVI < 0.55	Poor (V < 50%)	68	79	86	89
		Fair (50% < V < 75%)	49	69	79	84
		Good (> 75%)	39	61	74	80
Non-vegetated/ open space	NDVI < 0.31		69	84	88	91

Table 2 Initial CN_V values for vegetative cover

Soil type	CN_S	Class (HSG)
Loamy soil	86	B
Impervious/rocky surfaces	91	C

infiltration capacity is mostly insignificant, and hence, the value assigned for initial CN_{ISA} is 98. Composite CN value (Eq. 4) was finally assessed by summing the weighted average of the three components, viz. vegetation, ISA and soil (Fig. 7).

$$CN_C = ISA \times CN_{ISA} + V \times CN_V + S \times CN_S, \quad (4)$$

where ISA, *V* and *S* are the % of impervious surface, vegetation and soil, respectively; CN_C, CN_{ISA}, CN_V and CN_S denote composite CN, initial impervious surface CN, vegetation CN and soil CN, respectively. Subsequently, CN-II values were calculated for each sub-watershed in the study area.

Estimating surface runoff using NRCS-CN model

The NRCS model computes the direct runoff emanating from a watershed based on accumulated rainfall, initial abstraction and potential maximum retention. The potential

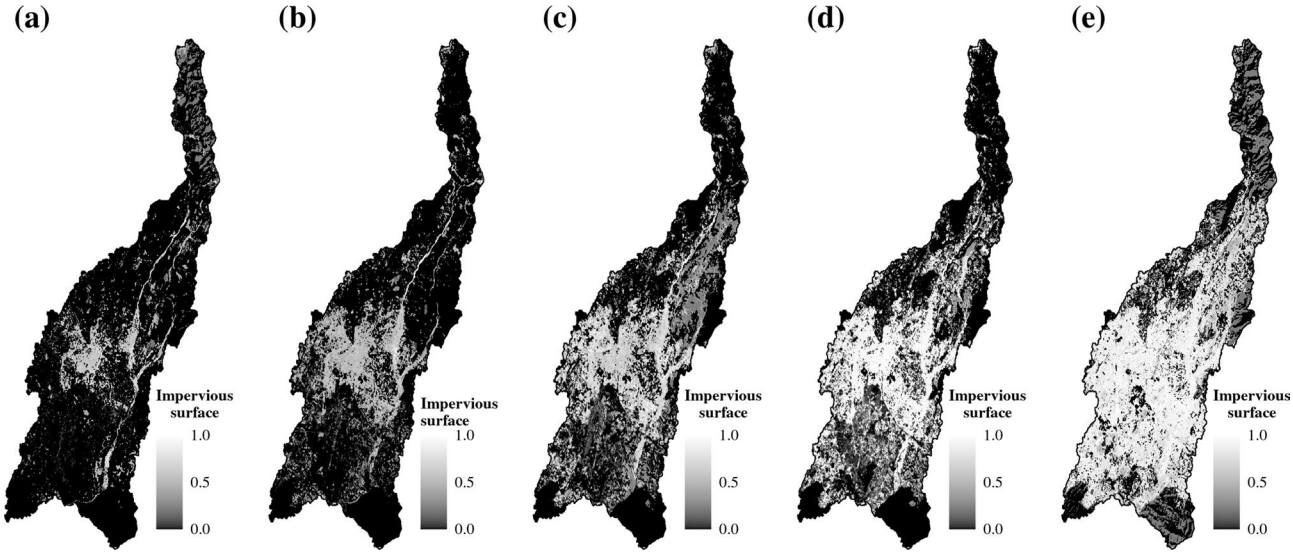

Fig. 4 Impervious surface fraction map **a** 1991 **b** 1998 **c** 2003 **d** 2011 and **e** 2018

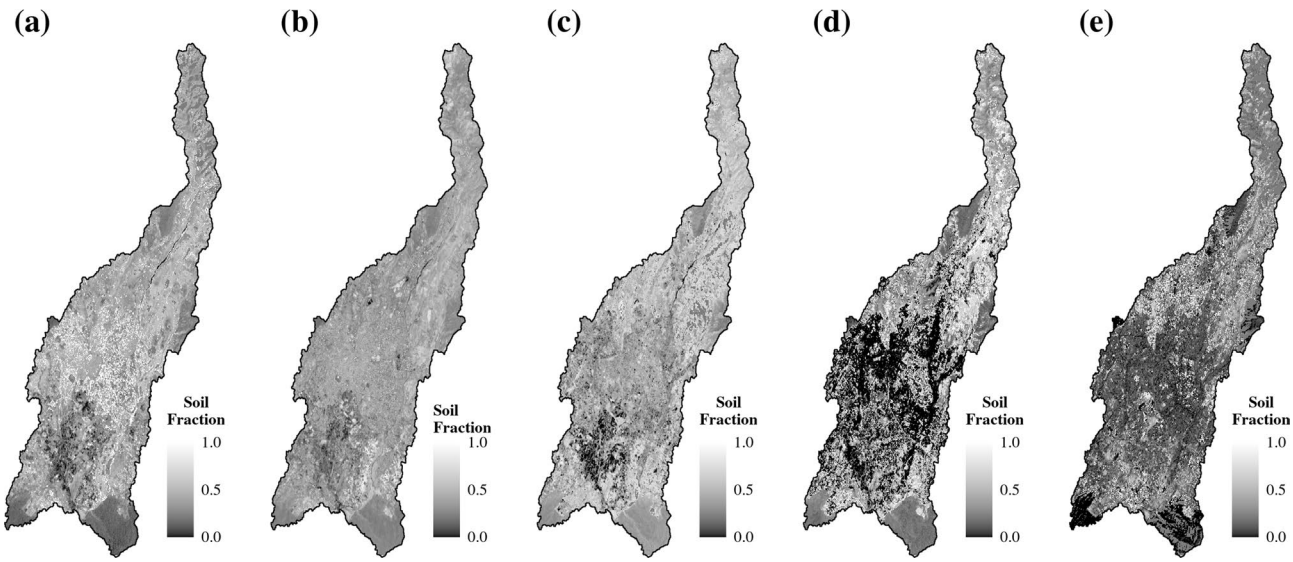

Fig. 5 Soil fraction map **a** 1991 **b** 1998 **c** 2003 **d** 2011 and **e** 2018

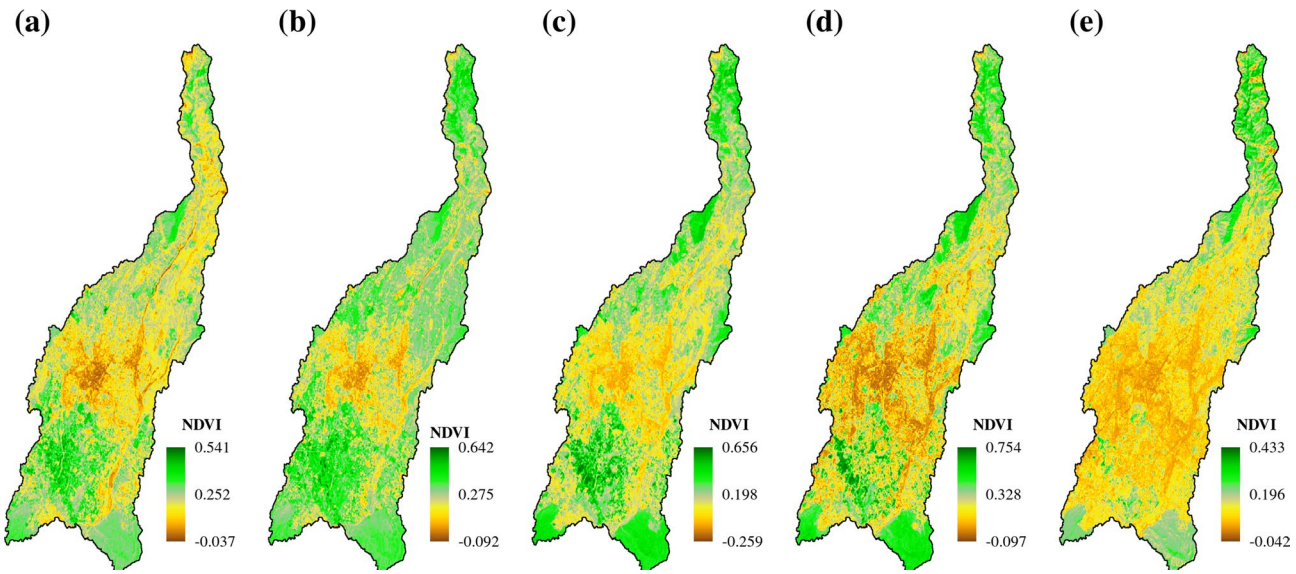

Fig. 6 NDVI **a** 1991 **b** 1998 **c** 2003 **d** 2011 and **e** 2018

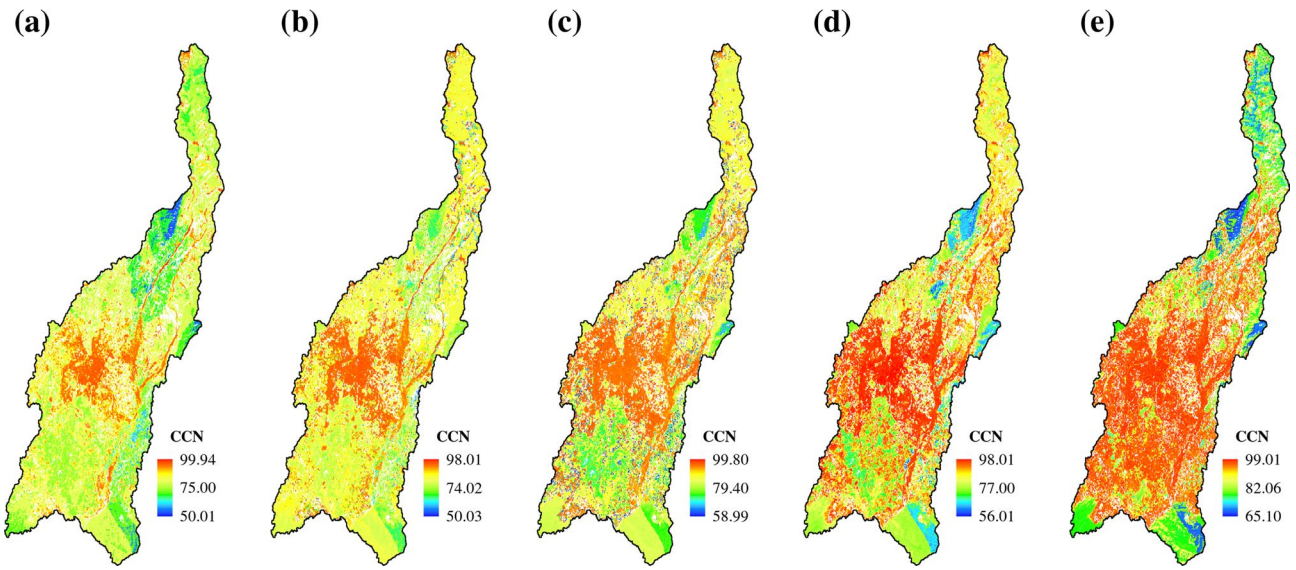

Fig. 7 Composite curve number map **a** 1991 **b** 1998 **c** 2003 **d** 2011 and **e** 2018

maximum retention is computed using CN table (SCS, 1986), which is a function of land use/ land cover (LULC) and HSGs. Using the NRCS model, the direct runoff is calculated (Eq. 5).

$$Q = \frac{(P - I_a)^2}{(P - I_a + S)}, \tag{5}$$

where Q is accumulated direct runoff in mm, P is accumulated rainfall depth in mm, I_a is initial abstraction in mm and S is potential maximum retention of water by soil over the catchment area in mm. The US Soil Conservation Service has described the $I_a = 0.2\,S$, while for Indian conditions, Eq. (5) is modified as described in Eq. (6) (Kumar et al. 1991) for AMC-III condition, and potential maximum retention (S) is mapped to the CN as given in Eq. (7):

$$Q = \frac{(P - 0.3S)^2}{(P - 0.7S)}, \tag{6}$$

$$S = 25.4\left(\frac{1000}{\mathrm{CN}} - 10\right). \quad (7)$$

The study region is situated in a hilly terrain, and hence besides the LULC, slope is also a driving factor for surface runoff. Slope correction was performed using Eq. (8) as defined by Huang et al. (2006):

$$\mathrm{CN_{cs}} = \frac{\mathrm{CN_c} \times (322.79 + 15.63 \times \mathrm{SL})}{\mathrm{SL} + 323.52}, \quad (8)$$

where $\mathrm{CN_{cs}}$ is slope corrected composite curve number, $\mathrm{CN_c}$ is composite curve number and SL is slope rise (in percentage).

The NRCS-CN is a dimensionless runoff index varying in the range 0–100, which demonstrates the ability of soil to allow infiltration of water through soil, within specific land use type and AMC. AMC is estimated based on rainfall characteristics of five-day period preceding a rainfall event. Accordingly, AMC-I, II and III levels are defined, which refer to dry, average or wet conditions, respectively, and correspond statistically to 90%, 50% and 10% cumulative probability of exceedance of runoff depth for a given rainfall event (Hjelmfelt et al. 1982). In the present study, the AMC-III condition was used which indicates the highest runoff potential of the soil, which practically happens when watershed areas are saturated from antecedent rains and lead towards water logging or urban floods.

Results and discussion

The study area is covered with built-up, scrub, fallow land and water bodies. The fringe areas of the study area are dominated with dense forest with fragmented spaces under built-up and road network. Diverse LULC types, pervious and impervious surfaces and soil conditions make the estimation of direct surface runoff a complicated task. Hence, the LSMA-derived V-I-S components were estimated for five years, i.e. 1991, 1998, 2003, 2011 and 2018. The sub-pixel analysis of impervious fraction map indicates that in the year 1991, the pixel value > 0.45 and in other representative years (1998, 2003, 2011 and 2018), values > 0.50 were observed to be impervious surface. Also, in some places new urban areas were developed in the form of colonies. Along the both sides of *Rajpur* road, the concentration of settlements has increased significantly. On the southern side of the study area around *Rispana* River, the residential colonies, namely *Mothrowala*, *Kedarpur*, *Chakshah Nagar*, etc., are the newly developed urban centres. In the year 2011 and 2018, the existing urban settlements were highly congested which led to the gradual formation of new settlements in the adjacent vacant land parcels. Also, the central part of the urban area is modified due to reconstruction of settlements and upcoming recreational centres. Consequently, the impervious surfaces have also increased due to gradual increases in urban settlements. More profound establishments can be seen developing around year 2003 on vacant lands, and densification can be observed around major roads while increasing the imperviousness and subsequent reduction in rainwater infiltration to the soil. This phenomenon has led towards frequent urban water logging and misery for urban dwellers. It was observed that there was > 500% increase in impervious area from 1991 to 2018 in the study area, considering a threshold of 0.45 (1991) and 0.50 (other years) for ISA fraction.

NDVI data offer a potential tool for vegetation categorisation. It was calculated using Landsat data for years 1991, 1998, 2003, 2011 and 2018, which indicate the progressive changes as demonstrated in Fig. 6. Overall, the NDVI values indicate the presence of healthy vegetation cover within the study area. It is observed that the mountainous tracts within the study area depict significantly higher NDVI values. In the southern side of study area, the *Pathri Bagh, Mothrowala,* etc. have relatively higher vegetal cover as these urban areas still have some land under cultivation. The vegetal cover has decreased in vicinity to *Amwala Karanpur* in the middle part of the watershed towards eastern direction where the vegetation fraction has changed from 0.5 to 0.34. In other dense forested areas of the watershed, the health and density of the natural vegetation has remained almost constant. During the years 1998 and 2003, the vegetal cover distribution has significantly changed mainly in peri-urban areas with the increasing built-up surfaces. Also, in the central part of the main urban centre, the urban green spaces were observed to be in a gradual degradation. Similar trend is also observed along the *Rajpur* road, where the vegetal cover is gradually degrading. The degraded vegetation cover shall expose the earth's surface and likely to cause higher surface runoff, water logging and flooding in urban areas. Considering the vegetation fraction, the study area showed an overall 76% decrease in vegetative fractional cover area (vegetation fraction with value > 0.45 considered) from 1991 to 2018.

The surface runoff from a watershed is a function of the soil types and their characteristics. On the basis of temporal image characteristics, the soil fraction maps for five different years have been estimated based on the methodology mentioned earlier. The index values of the soil fraction ranges between 1 (high) and 0 (low). The lower index values are observed in forested land which gradually goes higher in areas with bare soil. In the built-up areas, the soil fraction values are observed to be in a medium range. Interestingly, the areas in the vicinity of *Amwala*, *Karanpur*, *Khalanga* and *Danda Nooriwala* localities, the soil fraction index has got increased as cultivable agricultural lands have converted into fallow within this five-year span from 1998 to 2003. These peri-urban areas (during that period) are indicative of a trend where farmers leave the land as follow waiting

for prospective buyers/colonisers who create new urban settlements. Similarly, in the southern parts of the study area, mainly in vicinity to *Kedarpur*, *Mothrowala* and *Morowala*, the soil fraction values have decreased with the increasing settlement areas coming up within this zone. The accuracy assessment indicates a good agreement between ground and estimated results with RMSE for impervious surface as 0.24 and a bias of 0.14.

The corresponding CN values to that of impervious surfaces, vegetation and soil fractions indicate that areas with high fraction of ISA have positive correlation with CN values while the other two factors have a negative correlation with CN values. The increased ISA has resulted in reduced infiltration channels, thus raising the surface runoff as indicated through high CN values which is typically observed after year 1998. The values range from 60 (minimum) to 100 towards the maximum. The highest values are observed in the central part of the study area and quite evident near the major economic street of the city, i.e. *Rajpur Road* in northern part of Dehradun city.

Dehradun city experiences the highest amount of precipitation during the months of June to September owing to monsoon season. Eighty-seven per cent of the total rainfall is concentrated during this period with an annual average rainfall of 2183.5 mm. An extreme rainfall event of 149.3 mm (20 September 2010) based on daily rainfall data of 30 year (1982 to 2012) is considered to simulate surface runoff using improved NRCS-CN model embedded in HEC-HMS model. In the present study, only the monsoon months (June to September) have been considered in the study. The catchment area is divided into 146 sub-catchments for analysing the micro-scale dynamics of impact of urbanisation on runoff. The simulated runoff map in presented in Fig. 8. As per the HSG, the study area predominantly has moderately fine to coarse texture of sand and clay loam soil with moderately fine texture. The DEM-based slope and terrain conditions were also considered while simulating the runoff as it holds greater relevance for undulating terrain of the study area. On the basis of an extreme rainfall event, the surface runoff has been computed for all the 146 sub-watersheds for the five different selected years (1991, 1998, 2003, 2011 and 2018). The yearly analysis indicates higher surface runoff in the central and southern part of the city dominated by low vegetation and high impervious surfaces. Some areas in the central part of Dehradun city, namely *Chironwali*, *Karanpur*, *Nehru Colony, Subhash Nagar*, *and Shakti Enclave,* are very much vulnerable due to high surface runoff whereas other parts may also be affected if the rate of urban expansion remains uncontrolled. In the city core, the value of surface runoff has risen over the representative five years chosen for data analysis. In the year 2011 and 2018, the runoff has decreased in some areas of *Krishna Nagar* and *Garhi* Cantonment, as compared to year 2003 due to conversion of scrub land into grassland under the plantation drive programme. The main cause for the significant reduction in the surface runoff value in the southern part of the study area is that the fallow land were cultivated in the year 1998. In this study based on data availability, the data for year 1991 have been selected for January month whereas for other years the data are for March month. The *Rabi* crop is sown during October to December months; therefore, in January data, the tonal characteristics of green vegetation is lower in year 1991 as compared to images for other years. Overall, the average surface runoff has increased from 129.34 mm in 1991 to 140.02 mm in 2018 showing an overall increase of 8.25%. Figure 9 shows the distribution of runoff in the 146 sub-watersheds through a box and whisker plot.

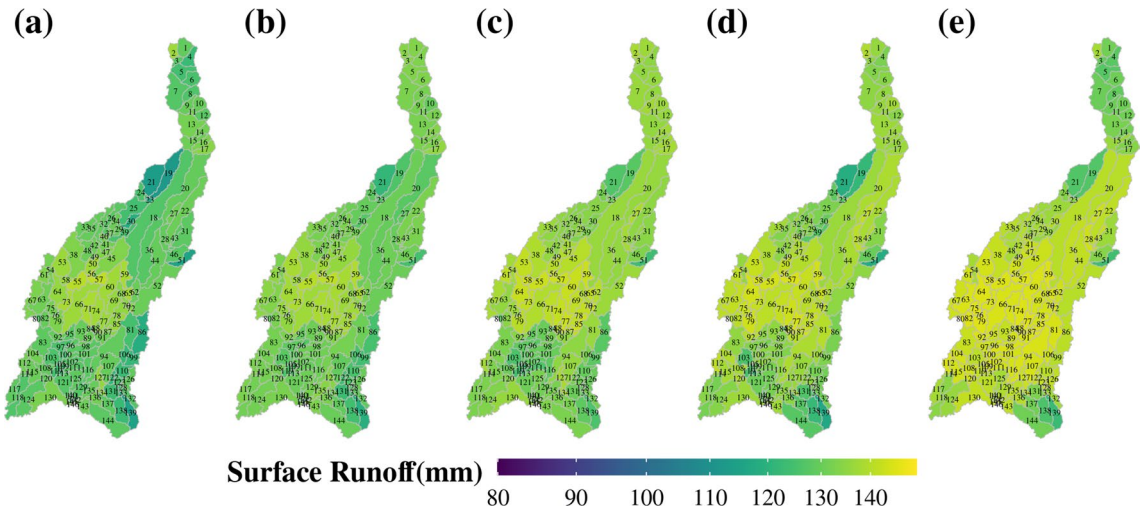

Fig. 8 Sub-watershed wise surface runoff for an extreme rainfall event of 149.3 mm for year **a** 1991 **b** 1998 **c** 2003 **d** 2011 and **e** 2018

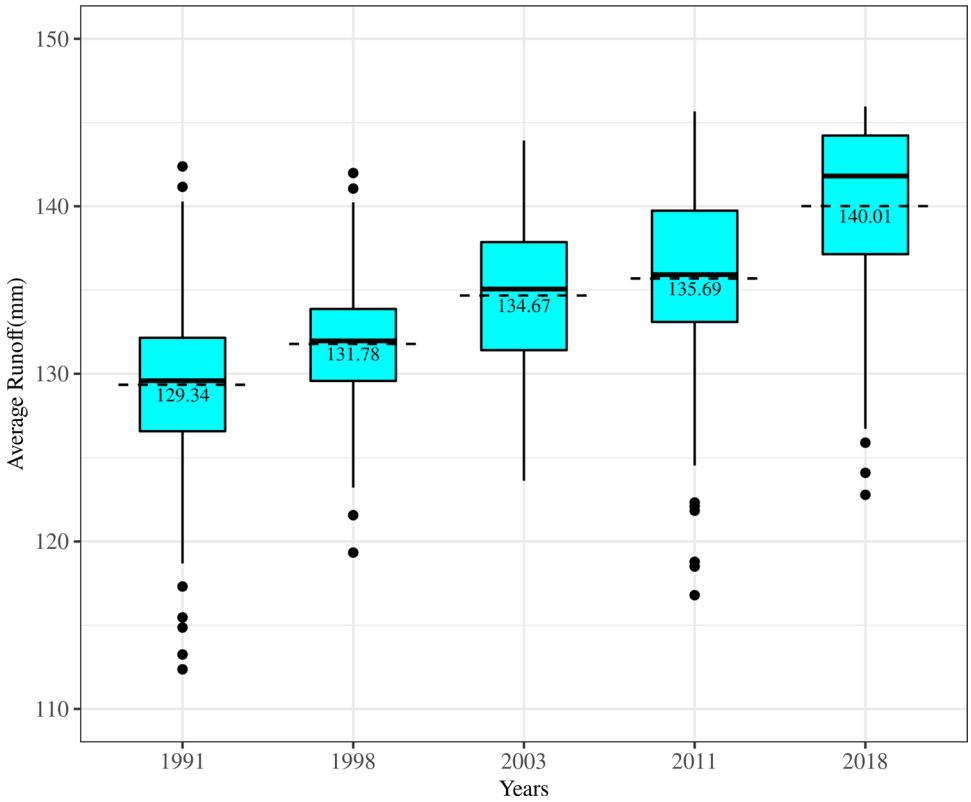

Fig. 9 Runoff distribution in the 146 sub-watersheds for different years

For the better assessment of the effect of imperviousness and vegetation on surface runoff in the urban areas, correlation between the parameters was established. In most of the cases, the sub-watersheds are experiencing increasing imperviousness and gradually decreasing vegetation cover. Also, some fallow lands have been converted into the settlement areas. The findings of the study imply that under an extreme rainfall event of 149.3 mm, a large area in central part of the city is vulnerable towards severe water logging or urban floods. A positive correlation is observed between surface runoff and ISA (R^2 varies between 0.62 and 0.89, $p < 0.05$), whereas inverse relationship is observed with vegetative cover in all sub-basins (R^2 varies between 0.61 and 0.91, $p < 0.05$) (see Figs. 10, 11).

Conclusions

Haphazard, unguided and unplanned urban growth may lead to several hydrological alterations. With high amount of rainfall, the natural landscape is degraded by the effects of soil erosion and exacerbated due to anthropogenic activities. In the urban environment, the situation is quite different than the other vegetated areas where infrastructure alteration happens rapidly. In the urban areas, the infiltration process due to rainwater is altered due to increase in impervious surfaces and degradation of the vegetal cover. Therefore, the rate of surface runoff will be quite high and that will favour the water logging and urban flooding.

Geospatial technology-based assessment of the urban surface runoff is gaining attention within the research fraternity due to its efficiency related to time and cost. In the present study, the peri-urban areas are witnessing growing population pressure as evident through increased settlement density. Based on the results obtained from imperviousness, vegetation and soil fraction analysis, overall changing scenario of the Dehradun city along with the surrounding areas has been observed. The degree of imperviousness of the urban landscape is growing rapidly with the expansion of urban built-up areas in the surrounding areas of the main urban centre. During the extreme event of rainfall, the urban areas experience high surface runoff leading to water logging and related urban flooding. The areas in vicinity to *Ballupur, Vivek Vihar, Chukkuwala, Karanpur, Laxman Chowk, Araghar, Panchapuri Colony, Nehru Colony, Rispana puram*, etc. are under gradually increasing surface runoff. Also, along the roadside areas near the *Rajpur, Jakhan, Chironwali*, etc. are getting converted into the settlements as well as into other

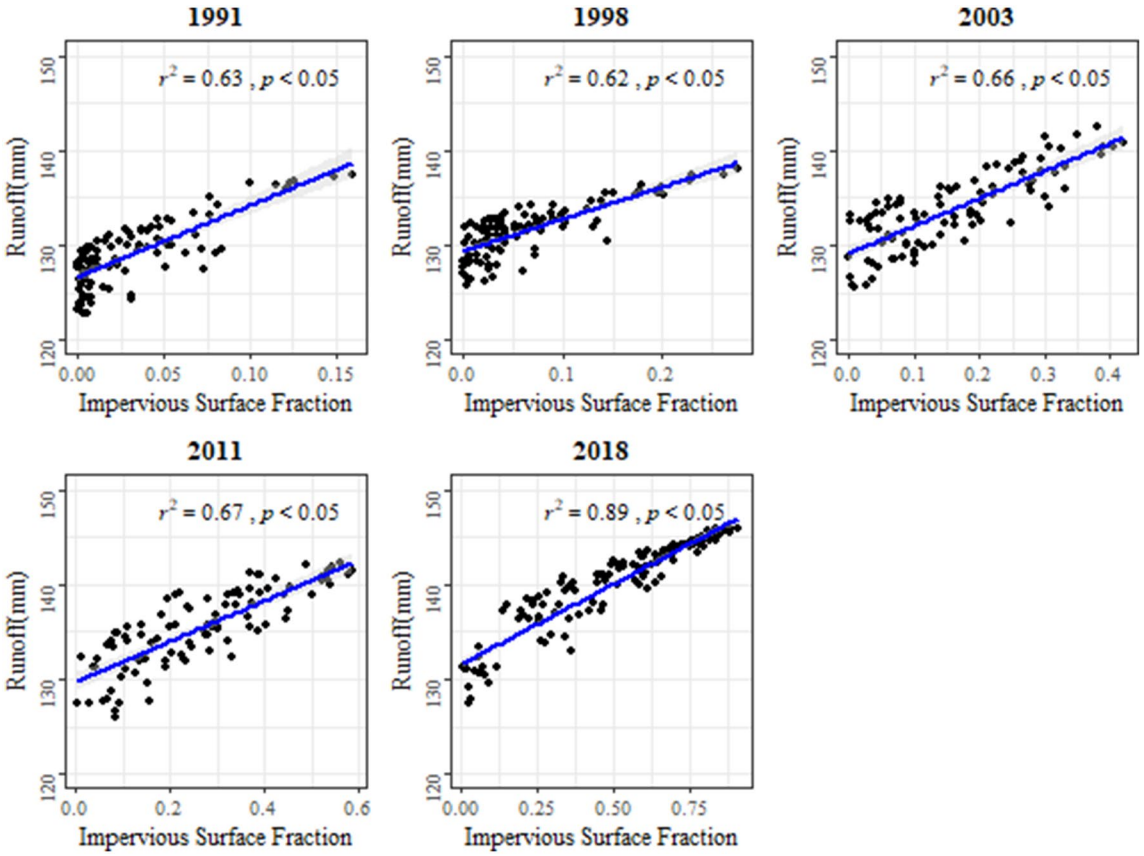

Fig. 10 Relationship between surface runoff (mm) and impervious surface area fraction for different years

impervious surfaces. Therefore, the surface runoff is increasing at a greater pace which may overwhelm the capacity of drainage systems. In other areas under forest, bare soil and scattered vegetated surfaces, the surface runoff conditions during the study period (1991, 1998, 2003, 2011 and 2018) have not varied much as observed for core urban areas. The findings of the study imply that under an extreme rainfall event of 149.3 mm, a large area in central part of the city is vulnerable towards severe water logging or urban floods. A positive correlation is observed between surface runoff and ISA (R^2 varies between 0.62 and 0.89, $p < 0.05$), whereas inverse relationship is observed with vegetative cover in all sub-basins (R^2 varies between 0.61 to 0.91, $p < 0.05$).

The NRCS-CN method utilising the benefit of sub-pixel analysis is a unique and relatively newer method for simulating surface runoff characteristics using V-I-S components. The composite CN calculated using V-I-S fraction maps help towards fragmenting the smaller hydrological unit, i.e. pixel into sub-pixel unlike studies concentrating on fewer dimension of land cover and vegetation only. Generally, the values based on localised conditions are neglected. Based on thorough ground knowledge about the study area, the critical part of assigning initial CN for all the three components was effectively accomplished.

The study reveals the efficacy of utilising the NRCS-CN method with inputs drawn from V-I-S fraction for runoff simulation and is an effective method for flood and flash flood monitoring and management. It also indicates that pervious surfaces have a greater role to play in minimising the runoff. Hence, controlled and guided urbanisation process can aid in mitigating the challenges posed by surface runoff from peak rainfall events causing frequent water logging or floods in urban areas.

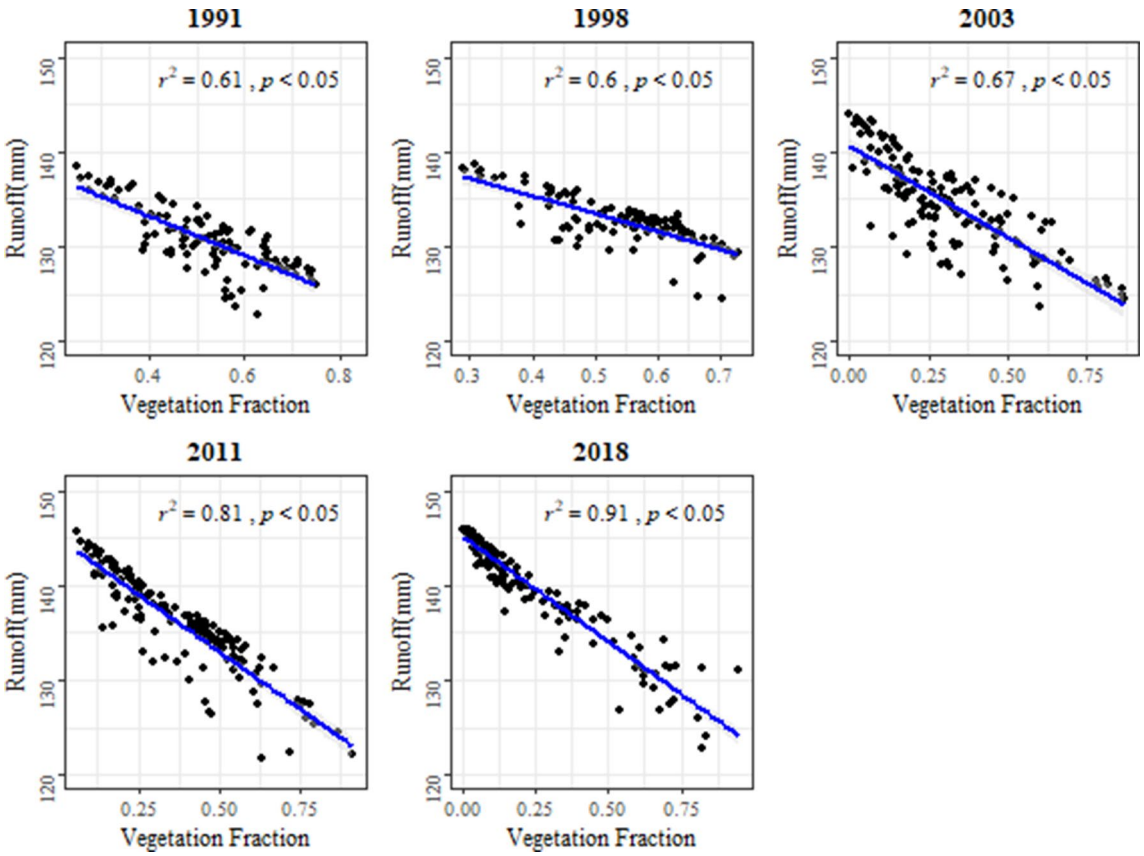

Fig. 11 Relationship between Surface runoff (mm) and Vegetation fraction for different years

Acknowledgements The authors would like to express their gratitude to the Director and Dean, Indian Institute of Remote Sensing, Dehradun, India, for their motivation to carry out research in applications of geospatial technology for resources management. We are thankful to editors and anonymous reviewers for their constructive comments and suggestions.

Funding No funding has been received to carry out the research.

Availability of data and material Mentioned in manuscript.

Compliance with ethical standards

Conflict of interest The authors declare no known competing financial interests or personal relationships that could have appeared to influence the work reported in the paper.

Ethical standards The research work is an original work and is submitted only to this journal.

References

Abdulkareem JH, Pradhan B, Sulaiman WNA, Jamil NR (2018) Review of studies on hydrological modelling in Malaysia. Model Earth Syst Environ 4:1577–1605. https://doi.org/10.1007/s40808-018-0509-y

Ajmal M, Moon GW, Ahn JH, Kim TW (2015) Investigation of SCS-CN and its inspired modified models for runoff estimation in South Korean watersheds. J Hydro Environ Res 9:592–603. https://doi.org/10.1016/j.jher.2014.11.003

Ajmal M, Waseem M, Ahn JH, Kim TW (2016) Runoff estimation using the NRCS slope-adjusted curve number in mountainous watersheds. J Irrig Drain Eng 142:04016002. https://doi.org/10.1061/(ASCE)IR.1943-4774.0000998

Al-Ghobari H, Dewidar A, Alataway A (2020) Estimation of surface water runoff for a semi-arid area using RS and GIS-based SCS-CN method. Water (Switzerland) 12(7):1924. https://doi.org/10.3390/w12071924

Arnold JG, Srinivasan R, Muttiah RS, Williams JR (1998) Large area hydrologic modeling and assessment part I: model development. J Am Water Resour Assoc 34(1):73–89. https://doi.org/10.1111/j.1752-1688.1998.tb05961.x

Bergstrom S (1995) The HBV model. In: Singh VP (ed) Computer models of watershed hydrology. Water Resources Publications, Highlands Ranch Co., USA, pp 443–476

Blaschke T, Hay GJ, Weng Q, Resch B (2011) Collective sensing: integrating geospatial technologies to understand urban systems—an overview. Remote Sens 3(8):1743–1776. https://doi.org/10.3390/rs3081743

Burnash, RJC (1995) The NWS river forecast system-catchment modeling. In: Singh VP (ed) Computer models of watershed hydrology. Water Resources Publications, Highlands Ranch Co., USA, pp 311–366

Cahyono C, Adidarma WK (2019) Influence analysis of peak rate factor in the flood events' calibration process using

HEC–HMS. Model Earth Syst Environ 5:1705–1722. https://doi.org/10.1007/s40808-019-00625-8
Caletka M, Šulc Michalková M, Karásek P, Fučík P (2020) Improvement of SCS-CN initial abstraction coefficient in the Czech Republic: a study of five catchments. Water (Switzerland) 12(7):1964. https://doi.org/10.3390/w12071964
Census of India (2011) Office of the Registrar General and Census Commissioner. Ministry of Home Affairs, Govt. of India. http://www.censusindia.gov.in. Accessed 27 Mar 2020
Downer CW, Ogden FL, Martin WD, Harmon RS (2002) Theory, development, and applicability of the surface water hydrologic model CASC2D. Hydrol Process 16(2):255–275. https://doi.org/10.1002/hyp.338
Dutta S, Mishra A, Kar S, Panigrahy S (2006) Estimating spatial curve number for hydrologic response analysis of a small Watershed. J Spat Hydrol 6(2):57–67
Fan F, Deng Y, Hu X, Weng Q (2013) Estimating composite curve number using an improved SCS-CN method with remotely sensed variables in Guangzhou. China Remote Sens 5(3):1425–1438. https://doi.org/10.3390/rs5031425
Fan F, Fan W, Weng Q (2015) Improving urban impervious surface mapping by linear spectral mixture analysis and using spectral indices. Can J Remote Sens 41(6):577–586. https://doi.org/10.1080/07038992.2015.1112730
Fortin JP, Turcotte R, Massicotte S et al (2001) Distributed watershed model compatible with remote sensing and GIS data. I: description of model. J Hydrol Eng 6(2):91–99. https://doi.org/10.1061/(asce)1084-0699(2001)
Gao GY, Fu BJ, Lü YH et al (2012) Coupling the modified SCS-CN and RUSLE models to simulate hydrological effects of restoring vegetation in the Loess Plateau of China. Hydrol Earth Syst Sci 16:2347–2364. https://doi.org/10.5194/hess-16-2347-2012
Gnecco I, Palla A, La Barbera P (2018) A dimensionless approach for the runoff peak assessment: effects of the rainfall event structure. Hydrol Earth Syst Sci 22(2):943–956. https://doi.org/10.5194/hess-22-943-2018
Gupta SK, Tyagi J, Sharma G et al (2019) An event-based sediment yield and runoff modeling using Soil Moisture Balance/Budgeting (SMB) method. Water Resour Manag 33(11):3721–3741. https://doi.org/10.1007/s11269-019-02329-1
Hjelmfelt AT Jr, Kramer KA, Burwell RE (1982) Curve numbers as random variables. In: Singh VP (ed) Computer models of watershed hydrology. Water Resources Publications, Highlands Ranch Co., USA, pp 365–370
Hörmann G, Köplin N, Cai Q, Fohrer N (2009) Using a simple model as a tool to parameterise the SWAT model of the Xiangxi river in China. Q Int 208(1–2):116–120. https://doi.org/10.1016/j.quaint.2008.11.007
Huang M, Gallichand J, Wang Z, Goulet M (2006) A modification to the Soil Conservation Service curve number method for steep slopes in the Loess Plateau of China. Hydrol Process Int J 20(3):579–589
Karunanidhi D, Anand B, Subramani T, Srinivasamoorthy K (2020) Rainfall-surface runoff estimation for the Lower Bhavani basin in south India using SCS-CN model and geospatial techniques. Environ Earth Sci 79(13):1–9. https://doi.org/10.1007/s12665-020-09079-z
Kousari MR, Malekinezhad H, Ahani H, Zarch MA (2010) Sensitivity analysis and impact quantification of the main factors affecting peak discharge in the SCS curve number method: an analysis of Iranian watersheds. Q Int 226(1–2):66–74. https://doi.org/10.1016/j.quaint.2010.05.011
Kowalik T, Walega A (2015) Estimation of CN parameter for small agricultural watersheds using asymptotic functions. Water (Switzerland) 7(3):939–955. https://doi.org/10.3390/w7030939
Kumar P, Tiwari KN, Pal DK (1991) Establishing SCS runoff curve number from IRS digital data base. J Indian Soc Remote Sens 19(4):245–252
Kumar S, Singh A, Shrestha DP (2016) Modelling spatially distributed surface runoff generation using SWAT-VSA: a case study in a watershed of the north-west Himalayan landscape. Model Earth Syst Environ 2(4):1–11. https://doi.org/10.1007/s40808-016-0249-9
Kumar V, Mohan A, Agarwal S, Siddiqui A (2019) Evaluating the close range hyperspectral data for feature identification and mapping. J Indian Soc Remote Sens 47:447–454. https://doi.org/10.1007/s12524-018-0889-5
Lu D, Weng Q (2006) Use of impervious surface in urban land-use classification. Remote Sens Environ 102:146–160. https://doi.org/10.1016/j.rse.2006.02.010
Lu D, Weng Q (2009) Extraction of urban impervious surfaces from an IKONOS image. Int J Remote Sens 30:1297–1311. https://doi.org/10.1080/01431160802508985
Lu D, Weng Q (2013) Spectral mixture analysis of the urban landscape in Indianapolis with Landsat ETM+ imagery. Photogramm Eng Remote Sens 70:1053–1062. https://doi.org/10.14358/pers.70.9.1053
Ludlow, CD (2009) Flood modeling in a data-poor region: A satellite data-supported model for Accra, Ghana. Doctoral dissertation The George Washington University
Meresa H (2019) Modelling of river flow in ungauged catchment using remote sensing data: application of the empirical (SCS-CN), artificial neural network (ANN) and hydrological model (HEC-HMS). Model Earth Syst Environ 5:257–273. https://doi.org/10.1007/s40808-018-0532-z
Nageswara Rao K (2020) Analysis of surface runoff potential in ungauged basin using basin parameters and SCS-CN method. Appl Water Sci 10(1):1–6. https://doi.org/10.1007/s13201-019-1129-z
Natarajan S, Radhakrishnan N (2019) Simulation of extreme event-based rainfall–runoff process of an urban catchment area using HEC-HMS. Model Earth Syst Environ 5:1867–1881. https://doi.org/10.1007/s40808-019-00644-5
Neitsch SL, Arnold JG, Kiniry JR, Williams JR (2011) Soil and water assessment tool theoretical documentation version 2009. Texas Water Resour Inst. https://doi.org/10.1016/j.scitotenv.2015.11.063
Pal SK, Majumdar TJ, Bhattacharya AK, Bhattacharyya R (2011) Utilization of Landsat ETM+ data for mineral-occurrences mapping over Dalma and Dhanjori, Jharkhand, India: An advanced spectral analysis approach. Int J Remote Sens 32:4023–4040. https://doi.org/10.1080/01431161.2010.484430
Phetprayoon T (2015) Application of GIS-based curve number method for runoff estimation in agricultural-forest watershed, Thailand. Asia Pac J Sci Technol 20:155–167
Psomiadis E, Soulis KX, Efthimiou N (2020) Using SCS-CN and earth observation for the comparative assessment of the hydrological effect of gradual and abrupt spatiotemporal land cover changes. Water (Switzerland) 12(5):1386. https://doi.org/10.3390/W12051386
Rajbanshi J (2016) Estimation of runoff depth and volume using NRCS-CN method in Konar catchment (Jharkhand, India). J Civ Environ Eng 6:4–9. https://doi.org/10.4172/2165-784X.1000236
Reistetter JA, Russell M (2011) High-resolution land cover datasets, composite curve numbers, and storm water retention in the Tampa Bay, FL region. Appl Geogr 31:740–747. https://doi.org/10.1016/j.apgeog.2010.12.005
Ridd MK (1995) Exploring a V-I-S (vegetation-impervious surface-soil) model for urban ecosystem analysis through remote sensing:

comparative anatomy for cities. Int J Remote Sens 16(12):2165–2185. https://doi.org/10.1080/01431169508954549

Roberts DA, Gardner M, Church R et al (1998) Mapping chaparral in the Santa Monica Mountains using multiple endmember spectral mixture models. Remote Sens Environ 65(3):267–279. https://doi.org/10.1016/S0034-4257(98)00037-6

Ruppert D, Shoemaker CA, Wang Y et al (2012) Uncertainty analysis for computationally expensive models with multiple outputs. J Agric Biol Environ Stat 17:623–640. https://doi.org/10.1007/s13253-012-0091-0

Samah A-J, Sharkh MA, Ziad A-M (2009) Estimation of runoff for agricultural watershed using SCS curve number and GIS. In: Thirteenth international water technology conference IWTC 13 2009. Hurghada, Egypt, pp 1213–1229

Shi W, Wang N (2020) Improved SMA-based SCS-CN method incorporating storm duration for runoff prediction on the Loess Plateau. China Hydrol Res 51(3):443–455. https://doi.org/10.2166/nh.2020.140

Sugawara M (1995) Tank model. In: Singh VP (ed) Computer models of watershed hydrology. Water Resources Publications, Highlands Ranch Co., USA, pp 165–214

US Army Corps of Engineers (2018) Hydrologic Modeling System HEC-HMS. User's Manual. Version 4.3. Hydrol Eng Centre

USDA Natural Resources Conservative Centre (1986) Urban hydrology for small watersheds. technical release No. 55. Washington D.C., United States. Government Printing Office

Velásquez-Valle MA, Sánchez-Cohen I, Hawkins RH et al (2017) Rainfall-runoff relationships in a semiarid rangeland watershed in central Mexico, based on the CN-NRCS approach. Model Earth Syst Environ 3(4):1263–1272. https://doi.org/10.1007/s40808-017-0379-8

Verma S, Singh PK, Mishra SK et al (2020) Activation soil moisture accounting (ASMA) for runoff estimation using soil conservation service curve number (SCS-CN) method. J Hydrol 589:125114. https://doi.org/10.1016/j.jhydrol.2020.125114

Wałęga A, Rutkowska A (2015) Usefulness of the modified NRCS-CN method for the assessment of direct runoff in a mountain catchment. Acta Geophys 63:1423–1446. https://doi.org/10.1515/acgeo-2015-0043

Walega A, Amatya DM, Caldwell P et al (2020) Assessment of storm direct runoff and peak flow rates using improved SCS-CN models for selected forested watersheds in the Southeastern United States. J Hydrol: Reg Stud 27:100645. https://doi.org/10.1016/j.ejrh.2019.100645

Weng Q (2012) Remote sensing of impervious surfaces in the urban areas: requirements, methods, and trends. Remote Sens Environ 117:34–49. https://doi.org/10.1016/j.rse.2011.02.030

Weng Q, Hu X (2008) Medium spatial resolution satellite imagery for estimating and mapping urban impervious surfaces using LSMA and ANN. IEEE Trans Geosci Remote Sens 46:2397–2406. https://doi.org/10.1109/TGRS.2008.917601

Wu C (2004) Normalized spectral mixture analysis for monitoring urban composition using ETM+ imagery. Remote Sens Environ 93:480–492. https://doi.org/10.1016/j.rse.2004.08.003

Wu C, Murray AT (2003) Estimating impervious surface distribution by spectral mixture analysis. Remote Sens Environ 84:493–505. https://doi.org/10.1016/S0034-4257(02)00136-0

Yang X, Liu Z (2005) Use of satellite-derived landscape imperviousness index to characterise urban spatial growth. Comput Environ Urb Syst 29(5):524–540

Yang J, He Y (2017) Automated mapping of impervious surfaces in urban and suburban areas: linear spectral unmixing of high spatial resolution imagery. Int J Appl Earth Observ Geoinf 54:53–64. https://doi.org/10.1016/j.jag.2016.09.006

Zhang H, Chen Y, Zhou J (2015) Assessing the long-term impact of urbanization on run-off using a remote-sensing-supported hydrological model. Int J Remote Sens 36:5336–5352. https://doi.org/10.1080/01431161.2015.109483